# Methanol electrosynthesis from $CO_2$ at $Cu_2O$/ZnO prompted by pyridine-based aqueous solutions

Jonathan Albo[a, c*], Garikoitz Beobide[b], Pedro Castaño[a] and Angel Irabien[c]

[a]*Department of Chemical Engineering, University of the Basque Country, Apdo. 644, 48080, Bilbao, Spain*

[b]*Inorganic Chemistry Department, University of the Basque Country, Apdo. 644, 48080, Bilbao, Spain*

[c]*Department of Chemical & Biomolecular Engineering, University of Cantabria, Avda. Los Castros s/n, 39005 Santander, Spain*

[*]Corresponding author; e-mail: jonathan.albo@unican.es

## Abstract

In this study we examine the electrochemical-driven reduction of $CO_2$ to methanol at $Cu_2O$/ZnO gas diffusion electrodes in soluble pyridine-based electrolytes at different concentrations. The process is evaluated first by cyclic voltammetric analyses and then, for the continuous reduction of $CO_2$ in a filter-press electrochemical cell. The results showed that the use of pyridine-based soluble co-catalysts lowered the overpotential for the electrochemical reduction of $CO_2$, enhancing also reaction performance (i.e. reaction rate and Faradaic efficiency). Reaction outcome is discussed on the basis of the role that N-ligands play on the mechanism and the inductive effect caused by the electron-releasing or electron-withdrawing substituents of the aromatic ring.

In particular, the maximum methanol formation rate and Faradaic efficiency reached at the 2-methylpyridine (with electron-releasing substituents)-based system with a pH of 7.6 and an applied current density of $j$= 1 mA·cm$^{-2}$ were $r$= 2.91 μmol·m$^{-2}$·s$^{-1}$ and $FE$= 16.86%, respectively. These values significantly enhance those obtained in the absence of any molecular catalyst ($r$= 0.21 μmol·m$^{-2}$·s$^{-1}$ and $FE$= 1.2%). The performance was further enhanced when lowering the electrolyte pH by adding HCl ($r$= 4.42 μmol·m$^{-2}$·s$^{-1}$ and $FE$= 25.6% at pH =5), although the system showed deactivation in the long run (5 h) which appears largely to be due to a change in product selectivity of the reaction (i.e. formation of ethylene).

**Keywords:** Electrochemistry, $CO_2$ reduction, pyridine-based molecular catalysts, copper oxide, methanol

## 1. Introduction

The idea that $CO_2$ can be captured [1-3] and reconverted to fuels in a Carbon Capture and Utilisation (CCU) approach, sounds like a perfect solution that potentially could help to solve global warming and energy shortage issues [4, 5]. Among the available technologies for the activation and conversion of $CO_2$ into value-added chemicals [6], the electrocatalytic alternative is appealing since it could enable an economically competitive industrial production of $CO_2$-based fuels by using renewable energy [7, 8].

Moreover, from the spectrum of possible $CO_2$-reduced species, the formation of methanol ($CH_3OH$) is of great interest since it is liquid at ambient conditions and can be readily integrated into the existing liquid fuel transportation infrastructure [9, 10]. However, an effective and selective production of $CH_3OH$ (with 6 exchanged $e^-$ required) by electrochemical methods is a chemical challenge that still remains unsolved. Despite the significant contributions that have been recently made in this reaction [9, 11-13], most of the $CO_2$ electroreduction reports have been largely confined to 2 $e^-$ products such as CO and formate (HCOOH) and, in many cases, with low productivities. Besides, even though proton-coupled electron transfers to $CO_2$ are thermodynamically facile, these reactions require large overpotentials [9]. In order to help solving those limitations, organic molecules have been found to be beneficial to promote the electrochemical reduction of $CO_2$ [14, 15]. In particular, nitrogen-containing heterocycles such as pyridine (Py) appear to lower overpotentials (indicating lower reaction barriers) and increase Faradaic efficiencies (indicating higher selectivities toward $CO_2$ reduction products) in electrochemical $CO_2$ conversion reactions as largely demonstrated by Bocarsly et al. [16-22]. Their first results evidenced that $CO_2$ is catalyzed at hydrogenated Pd electrodes in 10 mM aqueous Py solutions [19, 22]. $CH_3OH$ was detected with efficiencies up to 30% at overpotentials of uniquely ~200 mV [22]. Py was found to act as electron shuttle implying the formation of a carbamate as intermediate during the electron transfer to $CO_2$ [19]. In 2008, the same group exported this chemistry to a p-GaP photoelectrochemical cell to yield 96% Faradaic efficiency (*FE*) for $CH_3OH$. They showed evidence of the key role of Py to catalyze the selective formation of $CH_3OH$ from $CO_2$ in a series of one-electron steps at underpotentials of about 300 mV [21]. Based on the interesting results

for the electro-and-photoelectrocatalytic $CO_2$ reduction using Py developed by the group of Bocarsly, recent reports from other groups have been advancing on the application of Py-based molecular catalyst [23-29], demonstrating the benefits of using molecular catalysts for the reduction of $CO_2$ to $CH_3OH$.

While the mechanisms of the reduction process seem to be still subject of debate, the results clearly show that the identity of the soluble heterocycle and the metal electrode influences the yield and product selectivity of the reaction [23, 30-34]. For example, the use of Py with a p-GaP or a Pt cathode results in selective $CH_3OH$ formation, while Py with a Fe-pyrite cathode favours HCOOH production [15, 17, 22]. Among the available catalytic materials, copper has been found to be unique to synthesize $CH_3OH$ and >C1 hydrocarbons, such as ethanol and propanol [11-13, 35-37]. The performance of this metal, however, generally implies large overpotentials and low selectivities [38]. Nevertheless, copper(I) oxide surfaces (i.e. $Cu_2O$) present both intermediate hydrogen overpotentials and CO adsorption properties, which allows higher $CH_3OH$ yields in aqueous solutions to be produced [12, 13, 39-41]. Moreover, our previous work [13] demonstrated that ZnO is able to stabilize $Cu_2O$ in the hydrogenation reaction, maintaining the stability of the catalyst for longer reaction times.

Therefore, with the present study we sought to address the use of Py-based aqueous solutions for $CO_2$ conversion at $Cu_2O$/ZnO-based working electrodes. Previous works have pointed that N-donor ligands like pyridine play a crucial role in the electron transfer to $CO_2$ by forming a carbamate intermediate. Herein, a handful of pyridine derivatives were used in this study in order to assess the inductive effect caused by electron-releasing (*I*+) and electron-widthdrawing (*I*–) substituents into the overall reaction outcome. Precisely, we selected unsubstituted pyridine as reference and 2-methylpyridine, 4-ethylpyridine, 2,4,6-trimethylpyridine, 2-chloropyridine, and 4,4'-bipyridine as representative cases for *I*+ and *I*– effect. Influence of parameters such as Py type and its concentration was preliminarily addressed by cyclic voltammetry. Thereafter, continuous reduction of $CO_2$ to $CH_3OH$ was conducted in a filter-press electrochemical cell at low current densities ($j$= 0.01 - 5 mA·cm$^2$) in a pH range from ca. 7.6 to 4.

## 2. Materials and methods

### *2.1. Py-based molecular catalysts*

Pyridine (Py, 99%), 2-methylpyridine (2mPy, 98%), 4-ethylpyridine (4ePy, 98%), 2,4,6-trimethylpyridine (246tmPy, 99%), 2-chloropyridine (2ClPy, 99%), and 4,4'-bipyridine (44biPy, 99%) of reagent grade were used as commercially obtained. Figure 1 depicts the selected pyridines, together with the pKa values of the corresponding pyridinium. It must be noted that the pKa value can be correlated with inductive effect of the ring substituents. When compared to the unsubstituted Py, the alkyl derivatives (2mPy, 246tmPy and 4ePy) display an electron-releasing effect towards the N atom, making it a more basic position (i.e. a greater pKa of the pyridinium). 44biPy and 2ClPy exhibit somewhat lower and markedly lower pKa values according to their mild and strong electron-withdrawing effects. These features will be considered in the discussion section, as they are also closely related to the ability of the pyridinic ring to mediate the electron transfer through the formation of a carbamate intermediate by the nucleophilic addition to $CO_2$.

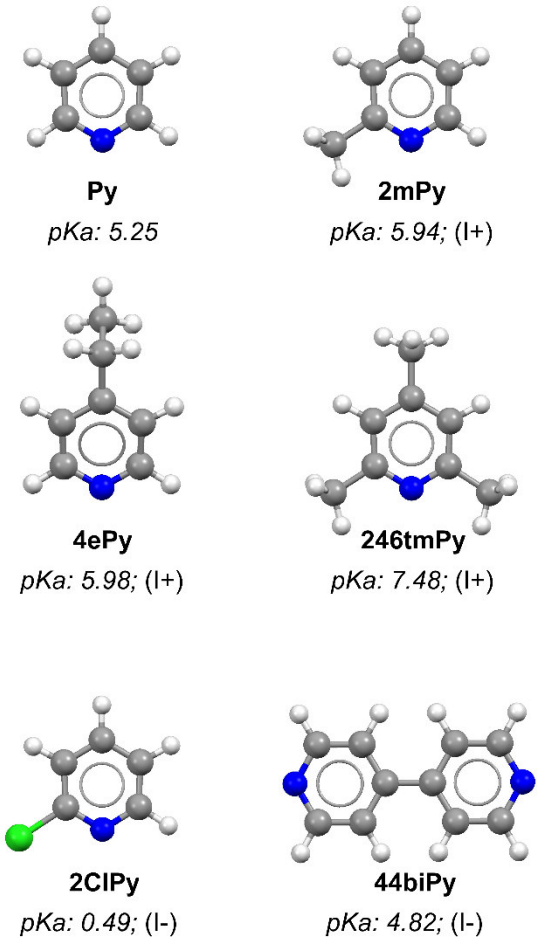


**Figure 1**. Selected pyridines (colour codes: C grey, H white, N blue, and Cl green) including pKa values of the corresponding pyridinium. Nature of the inductive effect in parentheses.

109

110 *2.2. Cyclic voltammetry characterization*

111 The electrochemical behaviour was evaluated with a PGSTAT 302N potentiostat
112 (Metrohm, Autolab B.V.) under GPES software control employing a conventional three
113 electrode electrochemical cell. A glassy carbon and Ag/AgCl (sat. KCl) were used as a
114 counter and reference electrode, respectively. Portions of the $Cu_2O$/ZnO-based materials
115 were used as cathodes. The aqueous electrolyte (0.5 M $KHCO_3$) containing the different
116 molecular catalysts at different concentrations (i.e. 10, 25 and 50 mM) was saturated with
117 ultrapure $CO_2$ (99.99%) by bubbling for 20 min before the tests. The current-voltages
118 curves were obtained with a scan rate of 50 $mV \cdot s^{-1}$ at potentials ranging from 0 to -1.2 V
119 vs. Ag/AgCl. Current density is expressed as the total current divided by the geometric
120 surface area, A, of the electrodes.

121 *2.3. Electrochemical cell for $CO_2$ reduction*

122 The continuous electrochemical measurements for $CO_2$ reduction were carried out in a
123 filter-press electrochemical cell (Micro Flow Cell, ElectroCell A/S) at ambient
124 conditions. A cation exchange membrane (Nafion® 117) separated the cathode and anode
125 compartments of the cell. The membrane presented a phase-segregated structure that
126 allows the selective transport of $H^+$ ions from the anode to the cathode chamber with a
127 low permeability to $CH_3OH$ [42]. A platinised titanium electrode was used as a counter
128 electrode and Ag/AgCl (sat. KCl), assembled close to the cathode, was used as reference
129 electrode. The $Cu_2O$/ZnO-catalyzed carbon papers were employed as working electrodes
130 (A= 10 $cm^{-2}$). The preparation of the $Cu_2O$/ZnO electrodes has been described in detail
131 in our previous works [12, 13]. Basically, $Cu_2O$ (Sigma Aldrich, particle size < 5 μm,
132 97% purity) and ZnO particles (ACROS organic, < 45 μm, 99.5%) were mixed with a
133 Nafion® dispersion 5 wt.% (Alfa Aesar) and isopropanol, IPA (Sigma Aldrich), with a
134 70/30 catalyst/Nafion mass ratio and a 3% solids (catalyst + Nafion). The ink was
135 airbrushed onto a porous carbon paper (TGP-H-60, Toray Inc.) to form a gas diffusion
136 electrode (GDE) with a catalytic loading of 1 $mg \cdot cm^{-2}$. All electrodes were dried and
137 rinsed with deionised water before use.

138 The filter-press electrochemical system possesses three inputs (catholyte, anolyte and
139 $CO_2$ separately) and two outputs (catholyte-$CO_2$ and anolyte). The GDE cell
140 configuration allows the electroreduction of $CO_2$ supplied directly in gas phase [12, 43,
141 44]. The cathode side of the reactor was fed with $CO_2$ gas (99.99%) with a flow/area ratio
142 of $Q_g/A$= 20 $ml \cdot min^{-1} \cdot cm^{-2}$, adjusted by a rotameter. A 0.5 M $KHCO_3$ (Panreac, >97%
143 purity) aqueous solution containing different concentrations of the Py-based molecular
144 catalysts (i.e. 10, 25 and 50 mM) was used as catholyte. The anolyte was a 0.5 M $KHCO_3$
145 aqueous solution. Prior to the experiments, the aqueous electrolyte was saturated with
146 $CO_2$ by bubbling for 20 min. The pH of the saturated solution was measured with a pH-
147 meter PH 25 (Crison, PAIS). The pH before the tests was adjusted to 4, 5 and 6 by adding
148 HCl (Panreac, 37%).

149 The electrolytes were pumped from catholyte and anolyte tanks to the cell by two
150 peristaltic pumps (Watson Marlow 320, Watson Marlow Pumps Group) at a flow rate of
151 $Q_e/A$= 1 $ml \cdot min^{-1} \cdot cm^{-2}$. The experiments were performed at galvanostatic conditions in a
152 current density range of $j$= 0.05 - 5 $mA \cdot cm^{-2}$, using an AutoLab PGSTAT 302N

potentiostat (Metrohm, Autolab B.V.) The experimental time was 90 min, where pseudo-stable conditions are reached [12, 13]. Liquid samples were taken every 15 min from the catholyte tank.

The concentration of products in each sample was analysed by duplicate in a headspace gas chromatograph (GCMS-QP2010 Ultra Shimadzu) equipped with a Flame Ionization Detector (FID). Compounds were separated on a DB-Wax 30 m x 0.25 mm x 0.25 µm column, with an injection and detector temperature of 250 ºC and 270 ºC, respectively. Helium was used as a carrier gas at a flow rate of 50 $ml \cdot min^{-1}$. The identification of obtained products was further confirmed by headspace gas chromatography-mass spectrometry (GCMS-N5975B) using a 60 m x 250 µm x 1.40 µm DB-624 capillary column. An averaged concentration was obtained for each point from the performance of three separate runs with an experimental error less than 17.3%.

The performance of the process is evaluated by the rate of $CH_3OH$ production, *r* (i.e. $CH_3OH$ obtained per unit of cathode area and time), and the *FE* (i.e. selectivity of the reaction to produce $CH_3OH$). *FE* is calculated assuming that 6 $e^-$ are required per molecule of $CH_3OH$.

## 3. Results and discussion

### *3.1. Cyclic voltammetric analyses*

Figure 2a reveals the current-voltage response after 5 electrochemical scans for the $Cu_2O$/ZnO GDEs in a $CO_2$-saturated 0.5 M $KHCO_3$ aqueous solution, and the response upon adding 25 mM concentration of 2mPy in the electrolyte solution. This Py-based co-catalyst was firstly selected due to its ability to significantly reduce the activation overpotential (i.e. its role in the activation energy due to electron transfer) for $CO_2$ reduction [45]. The results are compared to those responses obtained at a Cu plate. To further analyse the activity for $CO_2$ reduction, Figure 2b shows the curves for $Cu_2O$/ZnO and Cu electrodes under $CO_2$ and $N_2$ saturation. Current densities, *j*, are normalized to the geometric area (A) of the electrodes.

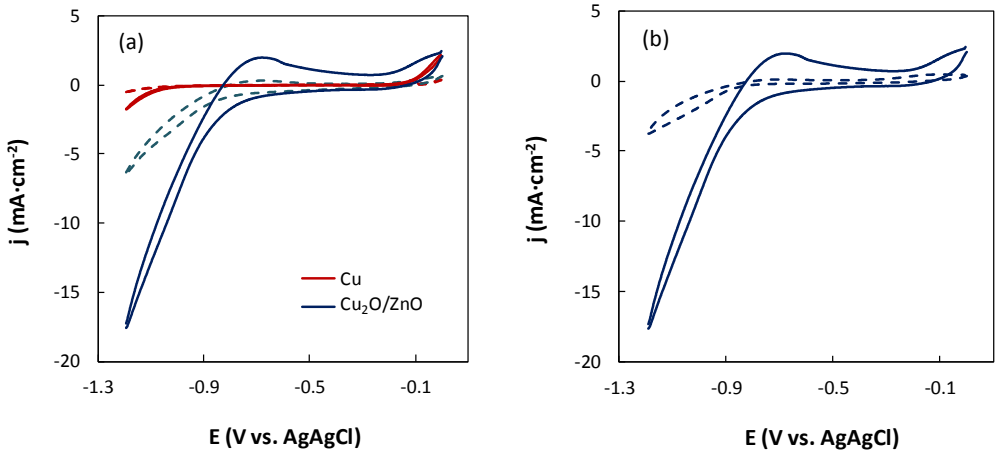


**Figure 2**. Cyclic voltammograms for: (a) $Cu_2O$/ZnO and Cu-based systems in $CO_2$-saturated 0.5 M $KHCO_3$ aqueous electrolytes in the presence and absence (dotted line) of 2mPy (25 mM) and, (b) $Cu_2O$/ZnO in $CO_2$ and $N_2$ (dotted line) saturated 0.5 M $KHCO_3$ + 2mPy (25 mM) solution.

Figure 2a shows that higher activities are reached for both Cu-based catalysts by employing Py-based molecular co-catalysts, as denoted by the large differences between voltammetry profiles in the absence/presence of 2mPy solubilised in the electrolyte. In fact, a very remarkable enhancement can be obtained in case of incorporating 25 mM of 2mPy in the $Cu_2O$/ZnO-based system, denoting the synergic co-catalytic effect of copper oxide species and Py in the activity response, in contrast with the restricted improvements at the Cu plate in the absence/presence of the molecular catalyst.

The main characteristic of the voltammograms is a reduction process starting at around -0.8 V vs. Ag/AgCl, which can be initially associated with the reduction of $CO_2$ and partial formation/decomposition of the oxides at the electrode surface. The oxidative peak at -0.7 V in the reverse scan of $Cu_2O$/ZnO curves might be initially assigned to the transition of remaining Zn to ZnO. However, the peak remains after the fifth scan, and so it probably has more to do with the formation of oxidized subproducts in the $CO_2$ reduction reaction. In addition, the curves in Figure 2b show that in the presence of both, 2mPy and $CO_2$, a substantial enhancement of the reduction wave, in comparison to that response in a $N_2$-saturated solution, was observed at more negative potentials than -1 V. Thus, this reduction peak is mainly attributed to $CO_2$ reduction rather than the oxidation-reduction of the catalytic materials. In fact, the reduction response occurs at around 200 mV lower overpotential in the presence of pyridine (compared to the system with a $CO_2$-saturated electrolyte without 2mPy). This denotes the important co-catalyst and synergic effect of 2mPy in the reduction of $CO_2$.

For the sake of evaluating the effect of the electron-releasing (*I*+) or electron-withdrawing (*I*-) character on $CO_2$ reduction activity, cyclic voltammograms were acquired for the other Py derivatives (i.e. 4ePy, 246tmPy, 2ClPy, 44biPy) in a concentration of 25 mM (Figure 3a). The results are compared to the electrochemical activity of unsubsituted Py as a reference. Besides, Figure 3b shows the effect of adding different concentrations of 2mPy (i.e. 10, 25 and 50 mM) in the $CO_2$ reduction response.

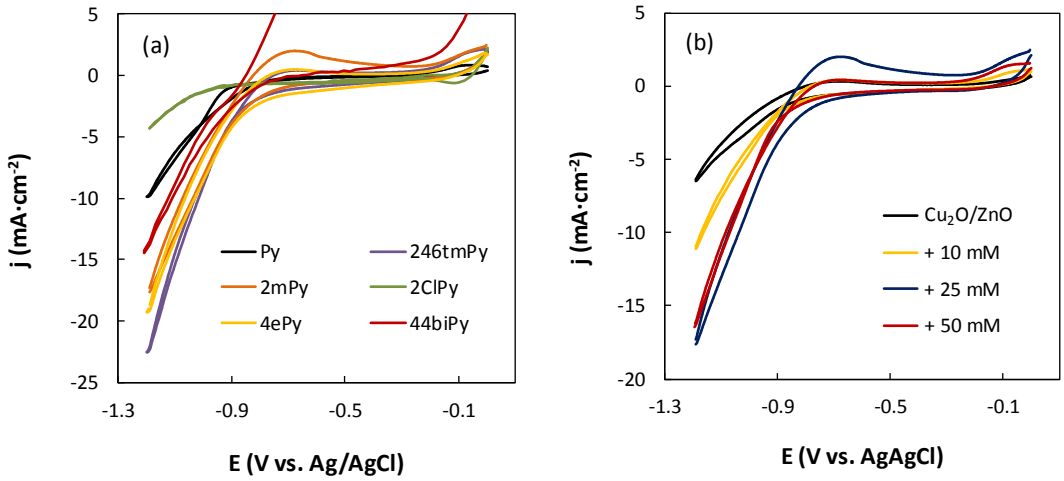


**Figure 3.** Cyclic voltammograms for $Cu_2O$/ZnO GDEs in a 0.5 M $KHCO_3$ aqueous solution containing: (a) 25 mM of the different Py-based molecular catalyst and, (b) different concentrations of 2mPy molecular catalyst (i.e. 10, 25 and 50 mM).

Compared to the reference Py, substituted ones show accused shifts on either onset of the reduction wave (i.e. lower activation overpotential) and its intensity. The lowering of the overpotential observed for 2mPy, 4ePy and 246tmPy can be rationalized by the electron releasing short alkyl groups (*I*+ effect). This makes the Py-N atom a better σ-donor and thus, more prone to form the carbamate through an addition reaction to the electrophilic C atom and, ultimately, to transfer the electron to $CO_2$.

On the contrary, the presence of a strong inductively electron-withdrawing group (*I*– effect) on the *orto* substituted 2ClPy, worsens σ-donor ability of N atom and hinders somewhat the formation of the carbamate and the resulting electron transfer. As a result, its voltammogram reveals a reduced current intensity and a shift towards greater overpotentials compared to referential Py. In the case of 44biPy, despite a slight worsening of the activity might be expected according to its moderate *I*– effect, its onset is somewhat lower than that of Py. Such behaviour might be attributed to the presence of two aromatic rings and two equivalent σ-donor N-atoms per molecule ready to transfer

two electrons. It is noticeably that the marked oxidation peak found for the voltammogram measured in presence of 44biPy points to the formation and subsequent oxidation of reduced intermediates different to those rendered by other pyrdinic co-catalysts (i.e. a change in selectivity). This fact can be also related to the ability of 44biPy to promote 2 e- transfer which would imply mechanistic changes (see Figure S1 in Supplementary information). In any case, apart of influencing in the $CO_2$ reduction, it must be considered that Py ring mediated electron transfer prompts also the catalytic generation of hydrogen [46], being also responsible of the reduction wave behaviour. This process follows also the above described trend, as the *I*+ effect caused by electron releasing groups leads to more basic N atom (higher pKa of the corresponding pyridinium), resulting in a molecular catalyst more prone to bind a proton and transfer the electron.

Moreover, Figure 3b demonstrated that with increases in Py ions in the solution, the catalytic current-response is enhanced up to a concentration of 25 mM. Further increases in concentration did not lead to higher voltammetric responses. Hence, the redox $CO_2$ reaction is limited by the high concentration of Py, suggesting that $CO_2$ has become the limiting reagent as the concentration of Py increases [18, 26].

*3.2. Filter-press electrochemical cell*

To further explore the performance of these co-catalysts, Table 1 presents the data for the continuous transformation of $CO_2$ in the filter press electrochemical cell equipped with a $Cu_2O$/ZnO GDE and the Py derivatives tested at different concentrations (i.e. 10, 25 and 50 mM) in the supporting electrolyte (0.5 M $KHCO_3$). The results are compared with those obtained in the absence of any Py molecular catalyst. The pH of the electrolytes ranged from 6.8 to 7.6 on dependence of the Py-based co-catalyst applied. The analysis is carried out in terms of *r* and *FE* at a low current density ($j$= 1 mA·cm$^{-2}$) where a better $CO_2$ electroreduction performance is expected in Py-based $CO_2$ co-catalyzed reactions [45].

The electroreduction process led to $CH_3OH$ formation, with also traces of $C_2H_5OH$, in accordance to previous results at copper oxides surfaces [9, 21, 22] and recent reports on the application of pyridines for $CO_2$ electroreduction [27-29]. No other liquid products were detected. Control experiments for the reduction of $CO_2$ at low overpotentials

catalyzed by the carbon paper (without sprayed $Cu_2O$/ZnO particles) did not produce any measurable liquid product.

**Table 1**. *r* and *FE* at $Cu_2O$/ZnO in the presence/absence of Py-based co-catalysts at different concentrations. $j$= 1 mA·cm$^{-2}$, $Q_e/A$= 1 ml·min$^{-1}$·cm$^{-2}$, $Q_g/A$= 20 ml·min$^{-1}$·cm$^{-2}$.

| ***Molec. Catalyst*** **(substituents)** | ***Py conc.*, mM** | ***E*, V vs. Ag/AgCl** | ***r*, μmol·m$^{-2}$·s$^{-1}$** | ***FE*, %** |
|---|---|---|---|---|
| - | - | -1.35 | 0.21 | 1.2 |
| Py | 10 | -1.21 | 2.6 | 15.06 |
| | 25 | -1.24 | 2.24 | 12.95 |
| | 50 | -1.17 | 0.94 | 5.42 |
| 2mPy (*I*+) | 10 | -1.03 | 2.91 | 16.86 |
| | 25 | -1.12 | 1.98 | 11.44 |
| | 50 | -1 | 1.46 | 8.43 |
| 4ePy (*I*+) | 10 | -1.02 | 1.35 | 7.83 |
| | 25 | -0.95 | 1.2 | 6.93 |
| | 50 | -1.14 | 0.73 | 4.22 |
| 246tmPy (*I*+) | 10 | -0.94 | 2.18 | 12.65 |
| | 25 | -0.99 | 2.24 | 12.95 |
| | 50 | -1.03 | 1.51 | 8.73 |
| 2ClPy (*I*-) | 10 | -1.41 | 0.73 | 4.22 |
| | 25 | -1.41 | 0.78 | 4.52 |
| | 50 | -1.15 | 0.42 | 2.41 |
| 44biPy (*I*-) | 10 | -1.16 | 0.26 | 1.51 |
| | 25 | -1.21 | 0.21 | 1.20 |
| | 50 | -1.19 | 0.16 | 0.90 |

The results indicated that by employing Py-based co-catalysts, an enhancement in $CH_3OH$ formation rates was observed in all cases, with values in general notably higher than those obtained at $Cu_2O$/ZnO GDEs in the absence of Py ($r$= 0.21 μmol·m$^{-2}$·s$^{-1}$) independently of the Py concentration applied. Besides, the cathodic voltages were in general more positive in case of adding Py-based molecular catalysts than those results in the absence of Py, being in concordance with the role that Py co-catalysts play in the electron transfer. For example, at an applied constant current of $j$= 1 mA·cm$^{-2}$ ($E$=- 1.03 V vs. Ag/AgCl), an averaged *FE* for $CH_3OH$ formation of 16.86% was observed with 2mPy (10 mM) as co-catalyst. Significantly higher voltage ($E$= -1.35 V vs. Ag/AgCl) was required under similar conditions in the absence of Py and only a *FE*= 1.2% was achieved. Moreover, the relative overpotential lowering follows the same trend that the one observed from cyclic voltammetric analyses (Figure 3a), according to the inductive effect caused by the substituents (see discussion in Section 3.1). Only 2ClPy shows an overpotential comparable to that provided by the $Cu_2O$/ZnO in the absence of co-catalyts,

indicating that electron-withdrawing effect caused by the $Cl^-$ substituent renders Py ring less active towards electron transfer (see above discussion).

As a rule, the lower voltages required in the Py-based co-catalysts are consistent with the faster kinetics to produce $CH_3OH$. The enhanced production rate is evident from comparison of $r = 2.91\ \mu mol \cdot m^{-2} \cdot s^{-1}$ obtained at 2mPy (10mM)-based system, which is an order of magnitude higher than $r = 0.21\ \mu mol \cdot m^{-2} \cdot s^{-1}$ in the absence of Py. Therefore, Py-based co-catalysts are able to reach higher *r* and *FE* at lower cathode potentials. Despite the relative low yields, the *FE* results are comparable to recent results (4-35%) for the use of pyridinium (protonated Py) and related aromatic nitrogen-heterocycles as electrocatalysts for $CH_3OH$ production [28, 29, 47-49]. Despite Py derivatives cause, in general, an improvement in *r* and *FE*, the results do not match the expectations considering only the inductive effect. For instance, the overpotential reduction caused by *I*+ substituents is not strictly correlated with the $CH_3OH$ production rate and Faradaic efficiency, since 4ePy and 246tmPy co-catalysts, possessing electron-releasing groups, reduce the overpotential with respect the unsubstituted Py, but lead to slightly worse *r* and *FE* values, which is probably due to the complexity of the multiple steps involved, stability of the intermediates and the formation of non-liquid subproducts [19, 46]. Further evidences are inferred from the case of 44biPy, that sets an overpotential comparable to referential Py, but leads to *r* and *FE* values as low as those provided in absence of co-catalyst. Again, such efficiency lowering is attributable to a change in product selectivity as previously inferred from the anomalous peak observed in the voltammogram for 44biPy (Figure 3a).

Increase in pyridine concentration from 10 to 25 mM led to a noticeable lower $CO_2$ conversion performance. These results are unexpected according to the higher $CO_2$ reduction activity observed from cyclic voltammetric analyses (Figure 3b), but agree well with previous observations, where redox $CO_2$ reactions were found to be limited at high concentrations of Py. Apparently, as pointed in the previous section, availability of $CO_2$ is the limiting factor, in such a way that an excess of Py co-catalyst can induce the catalytic generation of $H_2$ [46], resulting in lower *r* and *FE* for $CH_3OH$. In particular, a recent report for the photocatalytic reduction of $CO_2$ in Ru-phenanthroline complex photosensitizers, concluded that when Py concentration was higher than 6.35 mM, another unidentified redox reaction, apart from the conversion of $CO_2$ to $CH_3OH$, took place [50]. Further increases in molecular catalyst concentration led to a drastic reduction

in $CH_3OH$ yield and *FE*, which can be explained by a combination of $CO_2$ and proton reduction, the latter process dominating as the concentration of pyridinium increased [18]. Overall, the results denoted the benefits of using a $Cu_2O$/ZnO-Py-based system with an optimum molecular catalyst concentration of 10 mM for the electroreduction of $CO_2$, although the results for $CH_3OH$ concentration are limited to a sub-mg·$L^{-1}$ level, irrespectively of the Py-based co-catalyst concentration.

In order to identify kinetic limitations for $CH_3OH$ formation, Figure 4 presents the production rate and selectivity for $CH_3OH$ formation in a current density range of $j$= 0.05 - 5 mA·$cm^{-2}$ for the 2mPy (10 mM)-based system, where the best performance can be achieved.

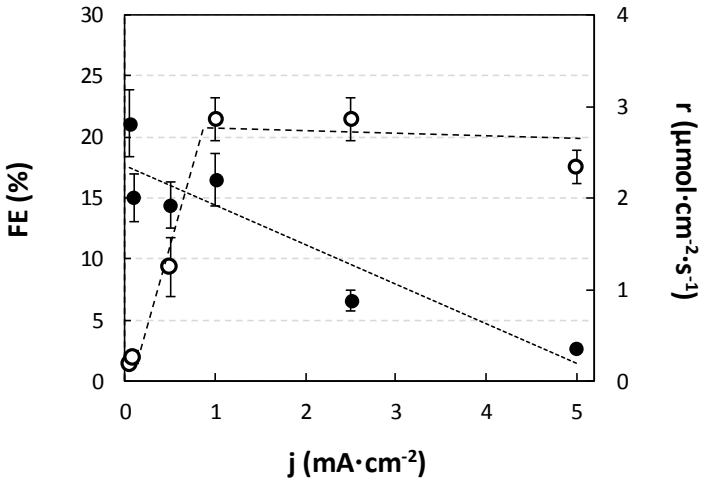


**Figure 4.** r(○) and *FE*(●) for $Cu_2O$/ZnO-2mPy (10 mM)-based system in a current density range of $j$= 0.05 - 5 mA·$cm^{-2}$.

The figure shows that *FE* for $CH_3OH$ generally increased as the current density lowered. The same was observed by Barton et al. [21] and Frese et al. [51], where *FE* for $CH_3OH$ increased as current density was reduced at Ga-based electrodes, due to the competing $H_2$ evolution in conjunction with $CO_2$ reduction. The same was recently reported by Rybchenko with Pt electrodes at high $CO_2$ pressure [27]. On the other hand, $CH_3OH$ production rate is remarkably reduced at low current densities ($j$= 0.05 - 0.5 mA·$cm^{-2}$) but then remains almost invariable at increasing currents ($j$= 1 - 5 mA·$cm^{-2}$), indicating a reaction-limited rate. Overall, with 2mPy as soluble electrocatalyst and a semi-optimum current density of $j$= 1 mA·$cm^{-2}$ the performance of the Py-co-catalyzed process seems to be enhanced.

328 *3.3. Influence of pH and long-term stability*

329 Previous literature demonstrated that $CO_2$ reduction is enhanced by pyridinum in aqueous
330 solutions of pH ranging from 5.2 to 5.4 [19, 22, 23, 29, 47, 49, 52], which can be related
331 to the pKa of Py [53]. It seems that at these pH conditions pyridinium exists in a higher
332 concentration than the free proton, enabling the Py to function as proton source ($[PyH^+]$)
333 as well as intermediates stabilizer via hydrogen bonding, enhancing also catalytic current
334 [26, 30]. Table 2 shows the quantitative information (*r* and *FE*) regarding the production
335 of $CH_3OH$ at a pH ranging from 4 to 6 in the $Cu_2O$/ZnO-2mPy (10 mM) system. The pH
336 was adjusted by adding HCl to the solution. Trace amounts of $C_2H_5OH$ were also
337 detected. The values are compared to the performance found at a pH of 7.6.

338 **Table 2**. *r* and *FE* at $Cu_2O$/ZnO-2mPy (10mM) for a pH range of 4 -7.6. $j$= 1 mA·cm$^{-2}$. $Q_e/A$= 1 ml·min$^{-1}$·cm$^{-2}$, $Q_g/A$= 20 ml·min$^{-1}$·cm$^{-2}$
339

| **pH** | ***E*, V vs. Ag/AgCl** | ***r*, µmol·m$^{-2}$·s$^{-1}$** | ***FE*, %** |
|---|---|---|---|
| 7.6 | -1.03 | 2.91 | 16.86 |
| 4 | -0.59 | 2.18 | 12.65 |
| 5 | -0.62 | 4.42 | 25.6 |
| 6 | -0.84 | 3.28 | 18.97 |

340

341 As observed, a mild acidification (pH= 5-6) led to increases in $CH_3OH$ production,
342 indicating that reaction kinetics depend on the concentration of pyridinium ions ($[PyH^+]$)
343 and/or hydrons available in the solution [26, 54, 55]. In fact, the marked lowering in the
344 overpotential points to a change in the reaction mechanism which necessarily needs to go
345 by a different transition state as the protonated pyridinium cannot directly form the
346 carbamate [19]. Specifically, the rate for $CH_3OH$ formation is as high as $r$= 4.42 µmol·m$^{-2}$·s$^{-1}$
347 at an optimum pH value of 5, which is around 1.5 times higher than the production
348 rate observed for $Cu_2O$/ZnO-2mPy (10 mM) at pH=7.6. In the same manner, the
349 efficiency of the process is significantly raised by reducing the pH of the solution, with a
350 value as high as *FE*= 25.6% for an applied voltage of $E$= -0.62 V vs. Ag/AgCl ($j$= 1
351 mA·cm$^{-2}$), thus corresponding to a overpotential of ca. 150 mV more than the
352 thermodynamic potential needed for $CH_3OH$ formation (-0.47 V vs. Ag/AgCl) at pH of
353 5.4 [22]. It is important to note that the reaction outcome improvement can be also
354 attributed to the partial dissolution of ZnO at mild acidic pHs, which would render more

$Cu_2O$ exposed at the surface of the cathode. It is also noteworthy to mention that this *FE* to $CH_3OH$ formation is comparable to that maximum value obtained in our previous report for the same $Cu_2O$/ZnO-based catalyst in the absence of any Py molecular catalyst ($FE_T$= 27.5%) [12], although in this latter a current density of $j$= 10 mA·cm$^{-2}$ was required. This indicates the relevance of using Py-based molecular catalysts to enhance the energy efficiency of the electrocatalytic reduction of $CO_2$.

Further reductions in pH to 4 produced a severe decrease in process efficiency, which could be initially interpreted by reductions in $CO_2$ solubility when decreasing the pH [18, 54]. Nonetheless, previous reports demonstrated the formation of copper(I) chloride (CuCl) in the presence of HCl when evaluating Cu-based electrocatalysts for $CO_2$ reduction [56]. CuCl compound has been proven to preferentially promote the formation of ethylene ($C_2H_4$) from the electrocatalytic reduction of $CO_2$, due to the ability of CuCl to reversibly combine with CO and $C_2H_4$ [56]. This will also explain the drastic reduction in *FE* to $CH_3OH$ observed at pH= 4.

Finally, an evaluation of the $Cu_2O$/ZnO-2mPy (10 mM)-based system performance for $CO_2$ electroreduction at ambient conditions is evaluated in the long-run (5 h). The results for *r* and *FE* evolution are presented in Figure 5a and Figure 5b in a pH of 7.6 and 5, respectively. The stability of the co-catalyzed reduction was tracked while continuously sparging the solution with $CO_2$ at a constant current density of $j$= 1 mA·cm$^{-2}$, where a good balance between *FE* and *r* is observed (Figure 4, Table 1).

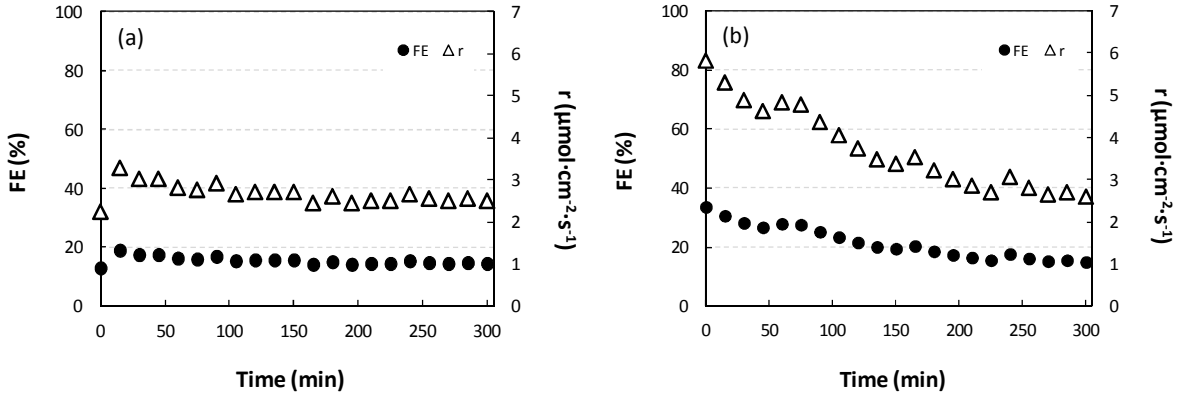


**Figure 5**. Time-dependence on *r* and *FE* for the $Cu_2O$/ZnO-2mPy (10 mM)-based system at (a) pH= 7.6 and (b) pH=5. $j$=1 mA·cm$^{-2}$, $Q_e/A$= 1 ml·min$^{-1}$·cm$^{-2}$, $Q_g/A$= 20 ml·min$^{-1}$·cm$^{-2}$.

As observed, the $Cu_2O$/ZnO-2mPy (10mM)-based system (pH= 7.6) showed only a slight activity decrease in the long run with a $CH_3OH$ formation rate of $r$= 2.5 μmol·m$^{-2}$·s$^{-1}$ and

*FE*= 14.45% at the end of the test (Figure 5a). We speculate that pairing a Py-based co-catalyst with a $Cu_2O$/ZnO cathode could potentially mitigate the limited stability observed in the electroreduction of $CO_2$ for $CH_3OH$ production [9]. In fact, previous literature demonstrated that a stable electroreduction of $CO_2$ to HCOOH over 5 days can be reached at Sn-2mPy-based electrocatalytic system for a current applied of $j$= 1 mA·cm$^{-2}$ in a membrane-separated cell [45]. In contrast, when the pH decreased to 5 (by the addition of HCl) a significant drop in process performance is clearly observed at the initial 3 h of experimental time with a 49% loss of activity (Figure 5b). Then, the production seems to slightly decrease (or stabilize) until the end of the test ($r$= 2.6 µmol·m$^{-2}$·s$^{-1}$, *FE*= 15.1%). In fact, the *FE* after 5 h is similar to that steady-state value observed for a pH = 7.6 (*FE*= 14.45%), which may probably indicate that the process performance is limited by the pyridine-$Cu_2O$/ZnO combination itself, rather than the pH of the electrolyte solution.

This reduction in process performance at pH= 5 is unexpected if we observe the stable $CH_3OH$ formation rates reached at long reactions times in photo-and-electrocatalytic systems based on Ga, Pd and Ru metals at a similar pH level [21, 25, 26]. For example, Barton et al. found that the production of $CH_3OH$ was linear with a charge passed ranging from 3 to 10 C at pH= 5.2 and 7 h of operation using a p-GaP-based photo-electrochemical cell. The Py concentration was also observed to be invariant over the time of the experiments, indicating that it is not consumed by the $CH_3OH$ formation reaction [21]. In the same manner, Wang et al. [26] observed a stable production of $CH_3OH$, as solo product, from $CO_2$ in aid of Ru-phenanthroline complex photosensitizer. The yield of $CH_3OH$ reached 60 µmol·L$^{-1}$ after 6 h of reaction time. Literature shows, however, that certain metals, such as Zn [57] and Cu [58], corrode more easily and give up electrodes when exposed to an acidic solution, which lead to a reduced performance. From our analyses a striking feature is that cathodic voltage rose only slightly after 5 h of electrolysis, from -0.62 V (after 15 min.) to -0.76 V vs. Ag/AgCl to maintain a current density of $j$= 1 mA·cm$^{-2}$ (Figure 5b). This limited increase in potential over time can be attributed to the consumption of the acid during the reduction process [47], since the pH of the aqueous electrolyte solutions increased from 5 to 5.69 after electrolysis. In any case, the limited increase in *E* probably indicate that the electrocatalytic system maintains its $CO_2$ reduction activity after 5 h of operation and thus, we hypothesized that the reduction in *r* and *FE* to $CH_3OH$ observed has probably more to do with a variation in product

411 selectivity ($C_2H_4$ formation with CuCl) [56], rather than the degradation of the catalytic
412 material in the presence of HCl. Overall, the stable formation of $CH_3OH$ at the
413 $Cu_2O$/ZnO-2mPy (10 mM)-based system at a pH of 7.6, with a *FE*= 14.45% and moderate
414 *r*= 2.5 $\mu mol \cdot m^{-2} \cdot s^{-1}$, show the potential of using Py-based molecular catalyst in the
415 electroreduction of $CO_2$ to $CH_3OH$.

416 The outstanding scientific challenge seems to be in the understating of the underlying
417 reaction mechanisms of Py-catalyzed $CO_2$ reduction processes to form $CH_3OH$, not only
418 to exhaustively elucidate the role of Py but also to develop related catalysts that exploit
419 the fundamental phenomena at play in the reduction reaction. It is suggested that the
420 reduction mechanisms of the reduction proceed through various coordinative interactions
421 between the Py radical and $CO_2$ to form carbamate-like species, which are proposed to be
422 the rate determining step for the process [18, 59], and then a subsequent sequential
423 electron and proton transfer processes to ultimately yield $CH_3OH$. In the current work,
424 the inductive effect caused by the electron-withdrawing and releasing substituents on σ-
425 donor N atom of the Py ring seems to play an important role in the electron transfer to
426 $CO_2$ and thus, in the reaction outcome. However, there is a delicate balance between
427 kinetics and thermodynamics underlying the observed reactivity. While increased
428 electron-releasing ability of the Py-based molecular catalyst is predicted to favour the
429 electron transfer to the electrophilic C atom of the $CO_2$ and increase reaction rate
430 corresponding to this stage, at the same time this would also stabilize the carbamate
431 species, which is not desired for the subsequent $CH_3OH$ formation [18]. Certainly, further
432 experimental work is required to fully elucidate $CO_2$ reduction steps to $CH_3OH$ in the Py-
433 based catalysed reaction, including the analysis of charge-transfer proccesses and the
434 governing physical and chemical phenomena taking place in the electrochemical systems
435 [60], although significant research efforts have been recently made [16, 26, 30-32, 54, 61-
436 66].

437 ## 4. Conclusions

438 This work demonstrated the beneficial use of pyridine-based molecular catalysts
439 containing electron-releasing or electron-withdrawing groups (i.e. 2-methylpyridine, 4-
440 ethylpyridine, 2,4,6-trimethylpyridine, pyridine, 2-chloropyridine, 4,4-bipyridine), to
441 reach enhanced energy efficiencies for the electrocatalytic reduction of $CO_2$ to methanol
442 at $Cu_2O$/ZnO-based surfaces.

443 The results showed that all the applied pyridine-based soluble co-catalysts lowered the
444 overpotential for the electrochemical reduction of $CO_2$. In particular, the reduction
445 response occurred at around 200 mV lower overpotential in the presence of 2-
446 methylpyridine (compared to the electrocatalytic system with a $CO_2$-saturated electrolyte
447 without it). The overpotential reduction with respect to the unsubstituted Py is explained
448 by electron-releasing alkyl groups (*I+ effect*) that makes the pyridinic ring more prone to
449 transfer an electron through a nucleophilic addition and consequent formation of a
450 carbamate intermediate.

451 The continuous electroreduction of $CO_2$ to methanol tests in a filter-press electrochemical
452 cell, showed a maximum methanol formation rate when using 2-methylpyridine (10 mM),
453 $r$= 2.91 $\mu mol \cdot m^{-2} \cdot s^{-1}$ (Faradaic efficiency= 16.86%), which is significantly higher than
454 that value in the absence of any molecular catalyst, $r$= 0.21 $\mu mol \cdot m^{-2} \cdot s^{-1}$ (Faradaic
455 efficiency= 1.2%). Importantly, process efficiency was significantly raised by reducing
456 the pH of the electrolyte to 5, with Faradaic efficiencies as high as $FE$= 25.6% for an
457 applied voltage of $E$= -0.62 V vs. Ag/AgCl ($j$= 1 $mA \cdot cm^{-2}$) in the 2mPy (10 mM)-based
458 system. This system, however, showed deactivation at longer reaction times, which may
459 be associated to a change in the selectivity of the reaction (i.e. formation of ethylene).

460 **Acknowledgements**

461 The authors gratefully acknowledge the financial support from the Spanish Ministry of
462 Economy and Competitiveness (MINECO), under the projects CTQ2013-48280-C3-1-R,
463 CTQ2014-55716-REDT and Juan de la Cierva program (JCI-2012-12073).

464 **References**

465 [1] Albo J., Yoshioka T., Tsuru T., Porous $Al_2O_3/TiO_2$ tubes in combination with 1-ethyl-
466 3-methylimidazolium acetate ionic liquid for $CO_2/N_2$ separation. Sep. Purif. Technol. 122
467 (2014) 440-448.

468 [2] Albo J., Irabien A., Non-dispersive absorption of $CO_2$ in parallel and cross-flow
469 membrane modules using EMISE. J. Chem. Technol. Biot. 87:10 (2012) 1502-1507.

470 [3] Albo J., Luis P., Irabien A. Carbon dioxide capture from flue gases using a cross-flow
471 membrane contactor and the ionic liquid 1-ethyl-3-methylimidazolium ethylsulfate. Ind.
472 Eng. Chem. Res. 49:21 (2010) 11045-11051.

473 [4] International Energy Agency (IEA). (2015). $CO_2$ emissions from fuel combustion:
474 Highlights.

475 [5] Aresta M., Dibenedetto A., Angelini A., Catalysis for the valorization of exhaust
476 carbon: From $CO_2$ to chemicals, materials, and fuels. Technological use of $CO_2$. Chem.
477 Rev. 114 (2014) 1709-1742.

478 [6] Centi G., S. Perathoner S., Opportunities and prospects in the chemical recycling of
479 carbon dioxide to fuels. Catal. Today. 148 (2009) 191-205.

480 [7] Martín A. J., Larrazábal G. O., Pérez-Ramírez J., Towards sustainable fuels and
481 chemicals through the electrochemical reduction of $CO_2$: lessons from water electrolysis.
482 Green Chem. 17 (2015) 5114-5130.

483 [8] Dominguez-Ramos A., Singh B., Zhang X., Hertwich E. G., Irabien A., Global
484 warming footprint of the electrochemical reduction of carbon dioxide to formate. J.
485 Cleaner Prod.104 (2015) 148-155.

486 [9] Albo J., Alvarez-Guerra M., Castaño P., Irabien A., Towards the electrochemical
487 conversion of carbon dioxide into methanol. Green Chem. 17 (2015) 2304-2324.

488 [10] Olah G. A., Goeppert A., Prakash G. K. S., Beyond oil and gas: the methanol
489 economy. Wiley-VCH, Weinheim, 2006.

490 [11] Albo J., Vallejo D., Beobide G., Castaño P., Cu-based metal-organic porous
491 materials for $CO_2$ electroreduction to alcohols. ChemSusChem. (2016).
492 doi: 10.1002/cssc.201600693.

493 [12] Albo J., Irabien A., $Cu_2O$-based catalysts for the electrochemical reduction of $CO_2$
494 at gas-diffusion electrodes. J. Catal. 343 (2016) 232-239.

495 [13] Albo J., Sáez A., Solla-Gullón J., Irabien A., Production of methanol from
496 $CO_2$ electroreduction at $Cu_2O$ and $Cu_2O$/ZnO-based electrodes in aqueous solution. Appl.
497 Catal. B-Environ. 176-177 (2015) 709-717.

498 [14] Lim R. J., Xie M., Ska M. A., Leea J-M., Fisher A., Wang X., Lim K. H. A review
499 on the electrochemical reduction of $CO_2$ in fuel cells, metalelectrodes and molecular
500 catalysts. Catal. Today. 233 (2014) 169-180.

[15] Oha Y., W. A. Organic molecules as mediators and catalysts for photocatalytic and electrocatalytic $CO_2$ reduction. Chem. Soc. Rev. 42 (2013) 2253-2261.

[16] Yan Y., Zeitler E. L., Gu J., Hu Y., Bocarsly A. B., Electrochemistry of aqueous pyridinium: exploration of a key aspect of electrocatalytic reduction of carbon dioxide to methanol. J. Am.Chem. Soc. 135 (2013) 14020-14023.

[17] Bocarsly A. B., Gibson Q. D., Morris A. J., L'Esperance R. P., Detweiler Z. M., Lakkaraju P. S., Zeitler E. L. Shaw T. W., Comparative study of imidazole and pyridine catalyzed reduction of carbon dioxide at illuminated iron pyrite electrodes, ACS Catal. 2 (2012) 1684-1692.

[18] Morris A. J., McGibbon R. T., Bocarsly A. B., Electrocatalytic carbon dioxide activation: the rate-determining step of pyridinium-catalyzed $CO_2$ reduction. ChemSusChem. 4 :2 (2011) 191-196.

[19] Barton C. E., Lakkaraju P. S., Rampulla D. M., Morris, A. J., Abelev, E., Bocarsly, A. B., Using a one-electron shuttle for the multielectron reduction of $CO_2$ to methanol: kinetic, mechanistic, and structural insights, J. Am. Chem. Soc. 132: 33 (2010) 11539-11551.

[20] Rosen B. A., Salehi-Khojin A., Thorson M. R., Zhu W., Whipple D. T., Kenis P. J. A., Masel R. I., Ionic liquid–mediated selective conversion of $CO_2$ to CO at low overpotentials, Science. 74: 2 (2009) 487-498.

[21] Barton C. E., Rampulla D. M., Bocarsly A. B., Selective solar-driven reduction of $CO_2$ to methanol using a catalyzed p-GaP based photoelectrochemical cell, J. Am. Chem. Soc. 130 (2008) 6342-6344.

[22] Seshadri G., Lin C., Bocarsly A. B., A new homogeneous electrocatalyst for the reduction of carbon dioxide to methanol at low overpotential, J. Electroanal. Chem. 372: 1-2 (1994) 145-150.

[23] Boston D. J., Xu C., Armstrong D. W., MacDonnell F. M., Photochemical reduction of carbon dioxide to methanol and formate in a homogeneous system with pyridinium catalysts. J. Am. Chem. Soc. 135: 44 (2013)16252-16255.

[24] Dongmei X., Magana D., Dyer R. B., $CO_2$ reduction catalyzed by mercaptopteridine on glassy carbon. J. Am. Chem. Soc. 2014, 136:40 (2014)14007-14010.

[25] Yang H., Qin S., Wang H., Lu J., Organically doped palladium: a highly efficient catalyst for electroreduction of $CO_2$ to methanol. Green Chem. 17 (2015) 5144-5148.

[26] Wang W., Zhang J., Wang H., Chen L., Bian Z., Photocatalytic and electrocatalytic reduction of $CO_2$ to methanol by the homogeneous pyridine-based systems. Appl. Catal. A-Gen. 520 (2016) 1-6.

[27] Rybchenko S., Touhami D., Wadhawan J, Haywood S., Study of Pyridine-Mediated Electrochemical Reduction of $CO_2$ to Methanol at High $CO_2$ Pressure. ChemSusChem. 9:13 (2016) 1660-1669.

[28] Yang H., Qin S., Yue Y., Liu L., Wang H., Lu J. Entrapment of a pyridine derivative within copper-palladium alloy: a bifunctional catalyst for electrochemical reduction of $CO_2$ to alcohols with excellent selectivity and reusability. Catal. Sci. Technol. 6 (2016) 6490-6494.

[29] Yang H., Yue Y., Qin S., Wang H., Lu J., Selective electrochemical reduction of $CO_2$ to different alcohol products by an organically doped alloy catalyst. Green Chem. 18 (2016) 3216-3220.

[30] Ertem M. Z., Konezny S. J., Araujo C. M., Batista V. S., Functional Role of Pyridinium during Aqueous Electrochemical Reduction of CO2 on Pt(111). J. Phys. Chem. Lett. 4: 5 (2013) 745-748.

[31] Lim C. H., Holder A. M., Musgrave C. B., Mechanism of homogeneous reduction of $CO_2$ by pyridine: proton relay in aqueous solvent and aromatic stabilization. J. Am. Chem. Soc. 135 (2013) 142-154.

[32] Keith J. A., Carter E. A., Theoretical insights into pyridinium-based photoelectrocatalytic reduction of $CO_2$. J. Am. Chem. Soc. 134: 18 (2013) 7580-7583.

[33] Keith J. A., Carter E. A., Electrochemical reactivities of pyridinium in solution: consequences for $CO_2$ reduction mechanisms. Chem. Sci. 4 (2013) 1490-1496.

[34] Yasukouchi K., Taniguchi I., Yamaguchi H., Shiraishi M. J., Cathodic reduction of pyridinium ion in acetonitrile. J. Electroanal. Chem. 105 (1979) 403-408.

[35] Qiao J., Liu Y., Hong F., Zhang J., A review of catalysts for the electroreduction of carbon dioxide to produce low-carbon fuels. Chem. Soc. Rev. 43 (2014) 631-675.

[36] Peterson A. A., Abild-Pedersen F., Studt F., Rossmeisl J., Nørskov J. K., How copper catalyzes the electroreduction of carbon dioxide into hydrocarbon fuels, Energy Environ. Sci. 3 (2010) 1311-1315.

[37] Gattrell M., Gupta N., Co A., A review of the aqueous electrochemical reduction of $CO_2$ to hydrocarbons at copper. J. Electroanal. Chem. 594 (2006) 1-19.

[38] Kuhl K. P., Cave E. R., Abram D. N., Jaramillo T. F., New insights into the electrochemical reduction of carbon dioxide on metallic copper surfaces. Energy Environ. Sci. 5 (2012) 7050-7059.

[39] Aeshala L. M., Uppaluri R. G., Verma A., Effect of cationic and anionic solid polymer electrolyte on direct electrochemical reduction of gaseous $CO_2$ to fuel. J. $CO_2$ Util. 3-4 (2013) 49-55.

[40] Le M, Ren M., Zhang Z., Sprunger P. T., Kurtz R. L., Flake J. C., Electrochemical Reduction of $CO_2$ to $CH_3OH$ at copper oxide surfaces. J. Electrochem. Soc.158: 5 (2011) E45-E49.

[41] Frese K. W., Electrochemical reduction of $CO_2$ at intentionally oxidized copper electrodes. J. Electrochem. Soc. 138: 11 (1991) 3333-3344.

[42] Heinzel A., Barragan V. M., A review of the state-of-the-art of the methanol crossover in direct methanol fuel cells. J. Power Sources. 84:1 (1999) 70-74.

[43] Del Castillo A., Alvarez-Guerra M., Irabien A., Continuous electroreduction of $CO_2$ to formate using Sn gas diffusion electrodes. AIChE J. 60:10 (2014) 3557-3564.

[44] Merino-García I., Alvarez-Guerra E., Albo J., Irabien A., Electrochemical membrane reactors for the utilisation of carbon dioxide. Chem. Eng. J. 305:1 (2016) 104-120.

[45] Parajuli R., Gerken J. B., Keyshar K., Sullivan I., Sivasankar N., Teamy K., Stahl S. S., Barton C. E., Integration of anodic and cathodic catalysts of earth abundant materials for efficient, scalable $CO_2$ reduction. Top. Catal. 58:1 (2015) 57-66.

585 [46] Baumgartel H., Retzlav K. J., Heteroaromatic Compounds. In Encyclopedia of
586 Electrochemistry of the Elements; Bard A. J., Lund H., Eds.; Marcel Dekker: New York,
587 1984; Vol. XV, p 194.

588 [47] Lee H. Q. J., Lauw S. J. L., Webster R. D., The electrochemical reduction of carbon
589 dioxide ($CO_2$) to methanol in the presence of pyridoxine (vitamin B6). Electrochem.
590 Commun. 64 (2016) 69-73.

591 [48] Cole E. E. B., Baruch M. F., L'Esperance R. P. L., Kelly M. T., Lakkaraju P. S.,
592 Zeitler E. L., Bocarsly A. B., Substituent effects in the pyridinium catalyzed reduction of
593 $CO_2$ to methanol: further mechanistic insights. Top. Catal. 58 (2015) 15-22.

594 [49] Portenkirchner E., Enengl C., Enengl S., Hinterberger G., Schlager S., Apaydin D.,
595 Neugebauer H., Knör G., Sariciftci N. S., A comparison of pyridazine and pyridine as
596 electrocatalysts for the reduction of carbon dioxide to methanol. ChemElectroChem. 1
597 (2014) 1543-1548.

598 [50] Ponnurangam S., Yun C. M., Chernyshova I. V., Robust electroreduction of $CO_2$ at
599 a poly(4-vinylpyridine)-copper Electrode. ChemElectroChem. 3 (2016) 74-82.

600 [51] Frese K. W., Canfield D., Reduction of $CO_2$ on n-GaAs electrodes and selective
601 methanol synthesis. J. Electrochem. Soc. 131:11 (1984) 2518-2522.

602 [52] Lebégue E., Agullo J., Morin M., Bélanguer D., The role of surface atoms in the
603 electrochemical reduction of pyridine and $CO_2$ in aqueous electrolyte.
604 ChemElectroChem. 1 (2014) 1013-1017.

605 [53] Hanai T., Koizumi K., Kinoshita T., Arora R., Ahmed F., Prediction of pKa values
606 of phenolic and nitrogen-containing compounds by computational chemical analysis
607 compared to those measured by liquid chromtography. J. Chromatogr. A. 762 (1997) 55-
608 61.

609 [54] Yuan J., Hao C., Solar-driven photoelectrochemical reduction of carbon dioxide to
610 methanol at $CuInS_2$ thin film photocathode. Sol. Energ. Mat. Sol. C. 108 (2013) 170-174.

611 [55] Appel A. M., Bercaw J. E., Bocarsly A. B., Dobbek H., DuBois D. L., Dupuis M.,
612 Ferry J. G., Fujita E., Hille R., Kenis P. J. A., Kerfeld C. A., Morris R. H., Peden C. H.
613 F., Portis A. R., Ragsdale S. W., Rauchfuss T. B., Reek J. N. H., Seefeldt L. C., Thauer

614 R. K., Waldrop G. L., Frontiers, opportunities, and challenges in biochemical and
615 chemical catalysis of $CO_2$ fixation. Chem. Rev. 113 (2013) 6621-6658.

616 [56] Ogura K., Yano H., Shirai F., Catalytic reduction of $CO_2$ to ethylene by electrolysis
617 at a three-phase interface. J. Electrochem. Soc. 150(9) (2003) D163-D168.

618 [57] Qi J., Zhang K., Ji Z., Xu M., Wang Z., Zhang Y., Dissolving behavior and electrical
619 properties of ZnO wire in HCl solution. RSC Adv. 5 (2015) 44563-44566.

620 [58] Sherif E-S. M., Corrosion behavior of copper in 0.50 M hydrochloric acid pickling
621 solutions and its inhibition by 3-amino-1,2,4-triazole and 3-amino-5-mercapto-1,2,4-
622 triazole. Int. J. Electrochem. Sci. 7 (2012) 1884-1897.

623 [59] Kamrath M. Z., Relph R. A., Johnson M. A., Vibrational predissociation spectrum
624 of the carbamate radical anion, $C_5H_5N\text{-}CO_2^-$, generated by reaction of pyridine with
625 $(CO_2)_m^-$. J. Am. Chem. Soc. 132 (2010) 15508-15511.

626 [60] Ehsani A., Mahjani M.G., Jafarian M., Naeemy A., Electrosynthesis of polypyrrole
627 composite film and electrocatalytic oxidation of ethanol. Electrochim. Acta. 71 (2012)
628 128‑133.

629 [61] Lim C-H., Holder A. M., Hynes J. T., Musgrave C. B., Reduction of $CO_2$ to methanol
630 catalyzed by a biomimetic organo-hydride produced from pyridine. J. Am. Chem. Soc.
631 136 (2014) 16081-16095.

632 [62] Keith J. A., Carter E. A., Theoretical insights into electrochemical $CO_2$ reduction
633 mechanisms catalyzed by surface-bound nitrogen heterocycles. J. Phys. Chem. Lett. 4
634 (2013) 4058-4063.

635 [63] Costentin C., Canales J. C., Haddou B., Saveant J. M., Electrochemistry of acids on
636 platinum. Application to the reduction of carbon dioxide in the presence of pyridinium
637 ion in water. J. Am. Chem. Soc. 135 (2013) 17671-17674.

638 [64] Lessio M., Cartes E. A., What is the role of pyridinium in pyridine-catalyzed $CO_2$
639 reduction on p‑GaP photocathodes? J. Am. Chem. Soc. 137 (2015) 13248-13251.

640 [65] Senftle T., Lessio M., Carter E., Interaction of pyridine and water with the
641 reconstructed surfaces of GaP(111) and CdTe(111) photoelectrodes: Implications for $CO_2$
642 reduction. Chem. Mater. 28:16 (2016) 5799-5810.

643 [66] Schneider T., Ertem M., Muckerman J., Angeles-Boza A., Mechanism of
644 Photocatalytic Reduction of $CO_2$ by $Re(bpy)(CO)_3Cl$ from Differences in Carbon Isotope
645 Discrimination. ACS Catal. 6 (2016) 5473-5481.